

NGC 4151: AN INTRINSICALLY AVERAGE SEYFERT 1

Andrzej A. Zdziarski,¹ Karen M. Leighly,² Masaru Matsuoka,³ Massimo Cappi,⁴ and Tatehiro Mihara⁵

ABSTRACT

We present a detailed analysis of a long, 100 ksec, observation of NGC 4151 by *ASCA*, contemporaneous with an observation by the *CGRO/OSSE*. We fit the data with physical models including an Fe K line and Compton reflection both relativistically broadened and coupled according to theoretical results. The model also includes a narrow Fe K component, which is emitted by both an extended plasma region and the X-ray absorber. Our study of the absorber shows strong evidence for the presence of more than one partial-covering cloud in the line of sight. Taking these points into account, our best intrinsic model includes a Comptonization continuum with an X-ray slope of $\Gamma \simeq 1.9$ from a thermal plasma with an electron $kT \sim 70$ keV and a disk line with an equivalent width of ~ 70 eV. The broadening of the line and reflection indicate their origin from innermost parts of an accretion disk. Our results indicate that NGC 4151 has an intrinsic X-ray spectrum and variability properties similar to those of average Seyfert 1s.

Subject headings: accretion, accretion disks — galaxies: active — galaxies: individual: NGC 4151 — galaxies: Seyfert — line: profiles — X-rays: galaxies

1. Introduction

NGC 4151, a Seyfert 1 galaxy at $z = 0.0033$, has the ~ 2 –10 keV photon index of its power-law component reported from observations by several different satellites to be in the range of $0.3 \lesssim \Gamma \lesssim 1.8$ (Yaqoob & Warwick 1991; Yaqoob et al. 1993; Wang et al. 1999, hereafter W99; Ogle et al. 2000; Yang et al. 2001; Piro et al. 2002). (Note that the lowest of these values, 0.3–0.4, have been measured by *Chandra*.) The corresponding average Seyfert 1 photon index is $\Gamma = 1.95$ with an intrinsic standard deviation of only 0.15 (Nandra & Pounds 1994), so the lower values in the above range are quite unusual. Since NGC 4151 is the

most often studied Seyfert (as it is the brightest one in the hard X-rays), it is of great interest to determine whether it is an archetype of its class or very far from it, as would be indicated by the spectral index varying up to 11σ from the average.

Reliable determination of the spectral indices of power law indices in accreting black holes is of major theoretical importance. Our present understanding of the power law component in both Seyferts and black hole binaries associates its origin with the process of thermal Comptonization (e.g., Poutanen 1998; Zdziarski 2000). However, this process yields in general $\Gamma > 1$ (e.g., Sunyaev & Titarchuk 1980). If, on the other hand, Comptonization were non-thermal, $\Gamma \geq 1.5$ (including cooling and pair production, e.g., Lightman & Zdziarski 1987). Very hard local continua can be obtained from Comptonization in a highly relativistic plasma ($kT \gtrsim 500$ keV) of a small optical depth (e.g., Haardt 1993), but this model for NGC 4151 is then in conflict with the measurement of its plasma temperature of $kT < 100$ keV (Johnson et al. 1997, hereafter J97; Zdziarski et al. 2000). If the measurement of $\Gamma \sim 0.3$ –0.4 in

¹Centrum Astronomiczne im. M. Kopernika, Bartycka 18, 00-716 Warszawa, Poland; aaz@camk.edu.pl

²Department of Physics and Astronomy, The University of Oklahoma, 440 W. Brooks St., Norman, OK 73019, USA; leighly@ou.edu

³NASDA-SURP 2-1-1, Sengen, Tsukuba, Ibaraki 305-8505, Japan

⁴Istituto Te.S.R.E, CNR, Via Gobetti 101, 40129 Bologna, Italy

⁵RIKEN, 2-1 Hirosawa Wako, Saitama, 351-0198, Japan

NGC 4151 (Ogle et al. 2000; Yang et al. 2001) is indeed confirmed, it would call for a new physical explanation. Furthermore, Yang et al. (2001) found no contribution of the scattered component to the soft excess in NGC 4151. However, this result was based on their value of $\Gamma = 0.3$ obtained assuming a single uniform absorber. On the other hand, the fitted value of Γ strongly depends on the model of the complex absorber in this source, as noted by Weaver et al. (1994, hereafter W94).

Also, the Fe K α line has been found to be very broad and strong in *ASCA* observations during hard states of NGC 4151 (Yaqoob et al. 1995; W99). A small Γ during those observations would constitute an interesting counterexample to the positive correlation between the strength and relativistic broadening of Fe K reprocessing features and Γ observed in Seyferts (Zdziarski et al. 1999; Lubiński & Zdziarski 2001), which is both expected theoretically and confirmed to hold in black-hole binaries (Gilfanov et al. 2000).

On the other hand, monitoring by the OSSE detector aboard *CGRO* shows the shape of its 50–300 keV spectrum to be weakly variable and very similar to the corresponding average spectra of Seyferts (J97; Zdziarski et al. 2000). In particular, the model of thermal Comptonization and Compton reflection (standard Seyfert continuum components) applied to the average OSSE spectrum of NGC 4151 yields the 2–10 keV index of $\Gamma \sim 1.9$ (J97), i.e., very close to the measured average of Seyfert 1s.

It is quite possible that the unusual properties of NGC 4151 noted above arise because the X-ray spectrum of NGC 4151 is usually strongly absorbed with a characteristic column density of $N_{\text{H}} \sim 10^{23} \text{ cm}^{-2}$, which makes measuring the intrinsic X-ray index difficult (as already noted by W94). For instance, the observation with the historical weakest absorption (Yaqoob et al. 1993), $N_{\text{H}} \sim 10^{22} \text{ cm}^{-2}$, has also the highest historical 2–10 keV flux, a soft $\Gamma \simeq 1.8$ and a low upper limit on the Fe K line (see also Zdziarski et al. 1996, hereafter Z96). This may indicate that an apparent correlation between the 2–10 keV flux and Γ (e.g., Yaqoob et al. 1993) is to a large degree due to strong absorption, which both suppresses the emitted X-ray flux and hardens the spectrum (although Yaqoob & Warwick 1991 have rejected that possibility based on their treatment of the absorp-

tion).

Z96 have suggested previously that the low values of Γ and/or the very strong Fe K line may be artifacts of insufficient account of complex absorption and neglect of Compton reflection. However, as noted by W99, the data used by Z96 were either of a low signal-to-noise ratio or limited energy resolution. Subsequently, W99 found the Fe K line to be very strong and broad and $\Gamma \simeq 1.3$ in a long, 100 ksec, *ASCA* observation in 1995, and commented on the unprecedented high signal to noise of that observation.

Here, we re-examine the above issues by re-analyzing the 1995 *ASCA* observation. Our treatment is different from that of W99, who considered only the 1–10 keV SIS data, as we analyze the full *ASCA* spectrum together with a contemporaneous OSSE observation and employ relatively more sophisticated physical models. Preliminary results of our study of the *ASCA* spectrum were given in Leighly et al. (1997, 1998). In our present best model, the intrinsic $\Gamma \simeq 1.9$, equal to that obtained from modelling the soft γ -rays. We conclude that previous reports of very low values of Γ in NGC 4151 are likely to be due to simplified treatments of the X-ray absorption and neglect of Compton reflection. We find the broad line to have a moderate equivalent width of $\sim 10^2 \text{ eV}$, which is average for Seyfert 1s with that Γ (Lubiński & Zdziarski 2001). Also, we find that the energy dependence of the variability amplitude implies a major role of complex variable absorption, in agreement with the results of the spectral fitting.

2. Data Analysis

NGC 4151 was observed by *ASCA* from 1995 May 10 02:49:43 till 1995 May 12 13:50:36 (UT, for the SIS) with the net exposure of $\simeq 10^5 \text{ s}$ for each of the detectors. SIS 1-CCD faint mode was used and standard data reduction was applied. Care was taken to exclude photons from the BL Lac object 1E1207.9+3945 (which lies 5' from NGC 4151), as shown in Figure 1. We have rebinned the original channels to 1/4 of the FWHM resolution of the SIS and GIS detectors, and assumed a 1.5% systematic error, which was estimated from residual discrepancies among the 4 *ASCA* detectors. We note that this observation was made only 2 years after the *ASCA* launch, and thus was only

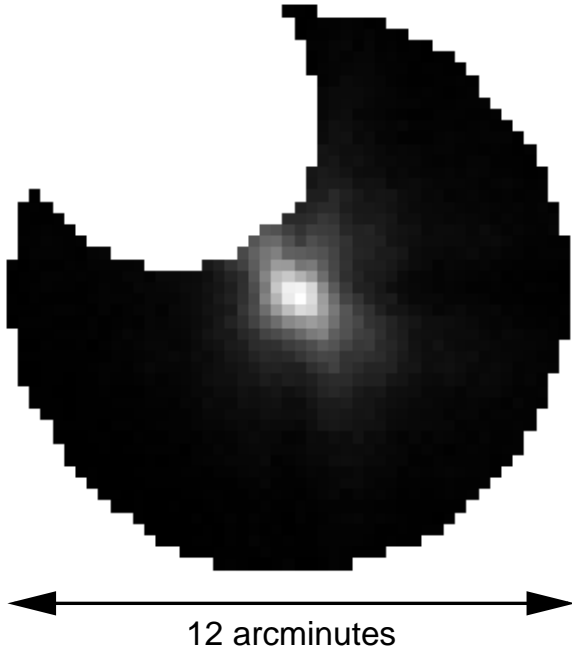


Fig. 1.— The part of the *ASCA* GIS2 image of the NGC 4151 used in the present reduction. The region around the nearby BL Lac 1E1207.9+3945 has been removed.

slightly affected by the time-dependent degradation of the SIS resolution.

We fit the data using XSPEC (Arnaud 1996). We assume elemental abundances from Anders & Ebihara (1982) and the interstellar Galactic absorbing column of $2.17 \times 10^{20} \text{ cm}^{-2}$ (Murphy et al. 1996). The single-parameter uncertainties below correspond to 90% confidence ($\Delta\chi^2 = 2.7$).

3. The Average Spectrum

3.1. Simple phenomenological models

We start with a model similar to one of those used by W94, consisting of a power law, assumed here to be e-folded with $E_c = 400 \text{ keV}$, absorbed uniformly with a column density, N_0 , and partially with a column N_1 covering a fraction f_1 (the so-called dual absorber). The soft component is modeled by the sum of a fraction, f_{sc} , of the power law scattering towards the observer (suffering only the Galactic absorption) and thermal bremsstrahlung. The model also includes a Gaussian Fe $K\alpha$ line absorbed only by the Galactic N_{H} , which is fitted to

be narrow with the width of $\sigma_n \simeq 0.1 \text{ keV}$ and the peak energy of $E_n \simeq 6.3 \text{ keV}$.

Such a model provided a good fit ($\chi^2/\nu \sim 1$) to the two $\sim 20 \text{ ksec}$ net-exposure data taken in 1993 (W94). However, it provides a very poor model to the present data, $\chi^2/\nu = 1016/641$, and it yields strong localized residuals, including one around $\sim 5\text{--}6.5 \text{ keV}$, as illustrated in Figure 2a. A likely reason for this difference is the much better statistics of the present data, which has a longer exposure by a factor of > 5 .

In particular, including (in addition to the narrow Gaussian) a broad Gaussian feature (absorbed as the power law) with the peak energy at $E_b = 5.9^{+0.1}_{-0.2} \text{ keV}$, the width of $\sigma_b = 0.9^{+0.2}_{-0.1} \text{ keV}$, and equivalent width of $W_b = 390 \text{ eV}$, reduces χ^2 by 141. Furthermore, the data show line-like residuals at 0.89 keV , and addition of a narrow line further reduces χ^2 by 123. This feature probably corresponds to the O VIII radiative recombination continuum and Ne IX emission that originates in the X-ray emitting narrow-line region, and is seen clearly in the *Chandra* spectrum (Ogle et al. 2000). Also, we find that the SIS continuum is systematically harder than the GIS one. This is likely to be due to the residual inaccuracy of the SIS calibration for the present very hard X-ray spectrum, and is recognized here because of the very good statistics. Addition of a small power law correction to the SIS model, $\Delta\Gamma$, reduces χ^2 by 41 (chance probability is 2×10^{-9} ; hereafter, we use the F-test to estimate significance of adding model components). Hereafter, we keep the soft line energy and $\Delta\Gamma$ fixed at 0.89 keV and $+0.047$, respectively. We note that W99, who analyzed the SIS data at energies $\geq 1 \text{ keV}$ only, have not considered the complexities of the soft spectrum present in the data.

This model, with $\chi^2/\nu = 711/637$, which is within $\sim 2\sigma$ of the mean of the χ^2 distribution, is formally acceptable but it has a number of problems. First, at the bremsstrahlung temperature of 0.31 keV , strong line emission is expected. However, using the *mekal* model in XSPEC (Mewe et al. 1985) actually worsens the fit by $\Delta\chi^2 = +16$. Second, the origin of the very strong and broad Gaussian line is unclear. It is indicative of very strong Compton reflection (e.g., Życki & Czerny 1994), which has not been included in the model. The continuum spectral

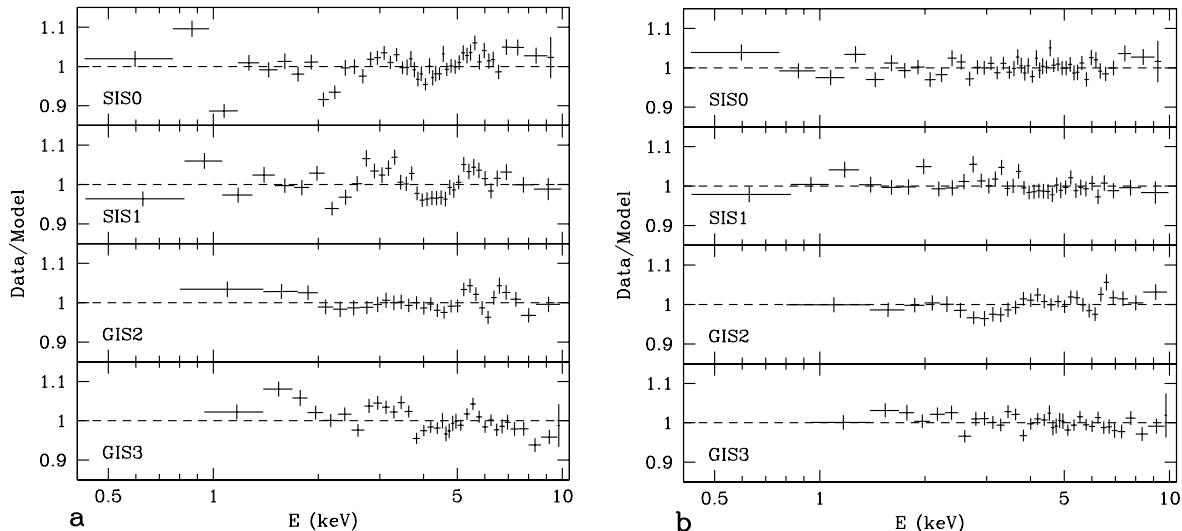


Fig. 2.— (a) The residuals to the model with a power law, dual absorber, a Gaussian line and bremsstrahlung. (b) The residual for our best model for the *ASCA* data, obtained by adding a disk line with associated reflection, ionization of the full screen, and an additional partially-covering cloud. (The assumed systematic error of 1.5% is not shown.)

index is $\Gamma = 1.39_{-0.05}^{+0.05}$, and Compton reflection is negligible in other Seyferts with a such a hard spectrum (Zdziarski et al. 1999). Thus, this model can be considered only an empirical (rather than physical) description of the spectrum.

3.2. Fe K line profile and Compton reflection

To make further progress, we have tried to develop a physical description of the spectrum by taking into account the following issues. The formation of Fe fluorescence lines proceeds through photoionization, so that the number of photons removed beyond the iron K-edge times the fluorescence yield equals the number of line photons. Broad Fe $K\alpha$ lines are most likely formed by reflection from a cold medium (Nandra & Pounds 1994). In this case, basic physics demands that the line flux should be tied to the relative strength of Compton reflection, $\Omega/2\pi$ (with the coefficient of proportionality dependent on the ionization state; George & Fabian 1991; Życki & Czerny 1994; Życki et al. 1998). Furthermore, if a line is broadened and shifted kinematically and by gravity, the same broadening will occur to the reflection component, in particular its K edge. Then, models with broad lines originating from illumination

of an accretion disk but either without reflection or with static reflection are not physically self-consistent.

We note that there is evidence that in some Seyferts with observed broad Fe K lines the simple model with irradiation of an accretion disk extending close to the minimum stable orbit may not be applicable (e.g., Chiang et al. 2000). Possibly, some of the red wings observed in Seyferts are due to a continuum complexity not understood at the present time rather than due to an irradiated accretion disk. On the other hand, the irradiated disk model, including the associated edge/reflection component, works well in some other cases, e.g., in the archetypical Seyfert 1 object IC 4329A (Done et al. 2000). In any case, a failure of the irradiated disk model cannot be considered a justification for fitting X-ray spectra with the disk line only and without the associated reflection component. Instead, new physical models for the red wings should be looked for.

The photoionization process preceding the Fe $K\alpha$ fluorescence should be neglected only when an edge/reflection component is so weak that it is observationally negligible. This is the case, in particular, for lines emitted by a Thomson-thin plasma (e.g., Makishima 1986). Such a narrow line is al-

ready included in our model, and it is due to both extended emission and the emission of the absorbing clouds. However, such lines are highly unlikely to be strongly Doppler/gravity broadened as an optically-thin accretion flow is necessarily very hot close to the central black hole (e.g., Narayan & Yi 1995; Abramowicz et al. 1995).

Accordingly, we replace the power-law continuum in the last model in §3.1 by the sum of a power law and Compton reflection normalized in such way that the line equivalent width with respect to the Compton-reflected component alone at 6.4 keV is $\simeq 1.3$ keV (George & Fabian 1991). This coefficient corresponds to a neutral or moderately ionized reflection, and we check this assumption *a posteriori* below. The reflection component (Magdziarz & Zdziarski 1995) is then Gaussian-broadened and redshifted in the same way as the line. The origin of the Gaussian broadening may be the chaotic motion of clouds in the vicinity of the black hole. This model yields a much softer intrinsic continuum, with $\Gamma = 1.87_{-0.10}^{+0.06}$, but very strong reflection, $\Omega/2\pi = 3.4_{-1.0}^{+0.7}$ ($W_b \simeq 390$ eV), at $\chi^2/\nu = 715/637$. We assumed here a face-on inclination; for a larger inclination, the fitted $\Omega/2\pi$ becomes even larger.

As noted in §3.1, Compton reflection as strong as this is unusual for Seyferts. Also, it is likely that accretion proceeds via a disk rather than clouds, and thus we consider the above model rather implausible. Therefore we replace the broad Gaussian line by a line from an accretion disk in the Schwarzschild metric with the rest energy of 6.4 keV and the emissivity $\propto r^{-\beta}$, extending from an outer radius, r_{out} (assumed here to equal 10^3) to an inner one, $r_{\text{in}} \geq 6$, where r is in the units of GM/c^2 (Fabian et al. 1989). The strength of the line is coupled to that of Compton reflection in the same way as above. The reflection spectrum is again relativistically broadened in the same way as the line (**refsch** in XSPEC). Since we include reflection, we constrain the inclination to $i \geq 15^\circ$, which corresponds to the range at which the reflection Green’s functions of Magdziarz & Zdziarski (1995) are valid.

The importance of including Compton reflection in models of reprocessing features is illustrated in Figure 3 for two cases with strong relativistic broadening in an accretion disk. We see that the effect is rather strong, and the reflection

component is by no means negligible. Also, taking into account the relativistic broadening of the reflection component is crucial. Roughly, the main effect of including relativistically-smearred reflection is an overall hardening of the total continuum, but without appearance of any distinct Fe K edge. The corresponding effect on the fitted parameters will be an increase of the fitted Γ of the incident spectrum.

We also include the $K\beta$ component (at the 7.06 keV rest energy and with the flux of 0.12 of that of $K\alpha$) for both the disk and the narrow lines. Also, we use the optically-thin plasma emission with the standard abundances (Mewe et al. 1985) instead of bremsstrahlung. This model yields $\chi^2/\nu = 701/636$, $\Gamma = 1.63_{-0.07}^{+0.04}$, $\Omega/2\pi = 1.34_{-0.29}^{+0.17}$ ($W_b = 160$ eV). The fit strongly prefers an inclination of the disk close to face-on, $i = 15^{+4^\circ}$, and emission of the reprocessed component concentrated close to the minimum stable orbit, $r_{\text{in}} = 6.2_{-0.2}^{+1.1}$, $\beta = 4.0_{-0.4}^{+1.4}$.

We note here that the quoted equivalent widths are given by XSPEC with respect to the continuum at the peak of the line. E.g., for models with $\beta \simeq 4.5$, $i = 15^\circ$, $r_{\text{in}} = 6$, this peak is at ~ 5.5 keV (Fig. 3b), at which the continuum photon flux is typically by $\sim 30\%$ higher than that at 6.4 keV. Thus, for the same photon flux of the line, the measured equivalent width will be correspondingly lower. This effect has to be taken into account when making comparison with theoretical results giving the line strength expected theoretically, which usually are expressed as the equivalent width of the line in the local rest frame (e.g., George & Fabian 1991; Życki & Czerny 1994).

3.3. Complex absorption

The complexity of absorption in NGC 4151 has long been appreciated (e.g. W94). Among others, Warwick et al. (1995) and George et al. (1998) have considered absorption by a partially ionized medium. However, W99 have found that this model provides a bad fit to the present data. On the other hand, ionization of the completely-covering component in the dual absorber model has been found to be required by Piro et al. (2002) for *BeppoSAX* data. We confirm their conclusion for our data, obtaining a reduction of χ^2 by 20 (the chance probability of 2×10^{-5}), a low ionization parameter of $\xi \simeq 0.6$ erg s $^{-1}$ cm, but only

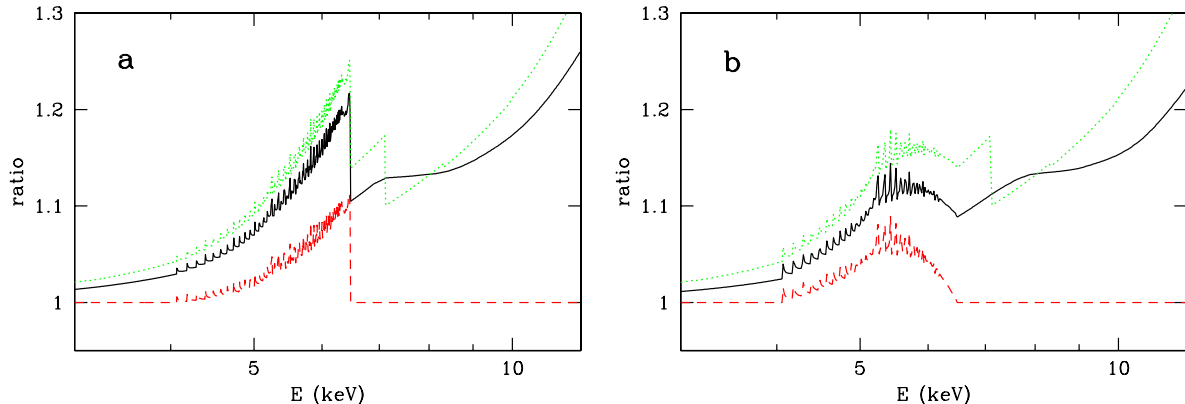


Fig. 3.— The effect of Compton reflection on the Fe $K\alpha$ disk line profile as illustrated by the ratio of the total spectrum to the incident power law with $\Gamma = 1.7$. The dashed curve shows the case with reflection neglected, the dotted curves show the line profile together with the associated reflection but neglecting its own relativistic smearing, and the solid curves give the correct spectrum in which both the line and the reflection components are relativistically smeared in the same way. The parameters are $r_{\text{in}} = 6$, $r_{\text{out}} = 10^3$, $i = 15^\circ$, $\Omega/2\pi = 1$ and (a) $\beta = 3$ and (b) $\beta = 4.5$. The wiggles in the line profile are numerical noise in the XSPEC implementation of the disk line in Schwarzschild metric (`diskline`, Fabian et al. 1989). We note that this numerical noise will be averaged out in data from *ASCA* given its resolution, but it prevents the `diskline` model from using in fits of high resolution data, e.g., those from *Chandra*.

small changes in the other fitted parameters. Here, $\xi \equiv 4\pi F_{\text{ion}}/n$, where F_{ion} is the ionizing flux, n is the reflector density, and the temperature of the reflecting medium is assumed to be 10^5 K (Done et al. 1992).

Next, we consider possible modifications of the partial covering component. Specifically, since there is no reason *a priori* that there should be a single partially-covering cloud in the line of sight, we investigate the possibility of multiple clouds in two ways. First, we replace the partial covering component by a Poisson distribution of clouds in the line of sight, first proposed by Yaqoob & Warwick (1991). However, this yields only a small increase of Γ and almost no change in χ^2 ; thus, it is not required statistically. Furthermore, the Poisson distribution requires an individual event to have small probability, and this distribution would not be appropriate if there are only a few clouds covering a substantial fraction of the source. Thus, we consider the case of just two partially covering clouds (with the column N_2 covering a fraction f_2 for the second one). This leads to our overall best model of the *ASCA* data, with $\chi^2/\nu = 655/633$. The probability that the fit improvement with respect to the previous model (the dual absorber

with a weakly ionized full screen, see above) is by chance is 4×10^{-6} . This model yields $i = 17_{-2}^{+3^\circ}$, $r_{\text{in}} = 6.3_{-0.3}^{+1.0}$, $\beta = 5_{-2}^{+2}$, and a much softer continuum, $\Gamma = 1.87_{-0.10}^{+0.07}$, $\Omega/2\pi = 1.20_{-0.37}^{+0.54}$ corresponding to $W_b = 110$ eV at the best fit. Interestingly, these Γ and Ω are close to the Seyfert average (Zdziarski et al. 1999). The residuals for this model are shown in Figure 2b.

3.4. The broad-band 0.4–400 keV spectrum

As noted in §1, the *ASCA* observation was nearly contemporaneous with an observation by OSSE, made 1995 Apr. 25–May 9. J97 has found that the variability of NGC 4151 in soft γ -rays is rather slow and modest. Thus, we fit the OSSE spectrum (at a free relative normalization) together with the *ASCA* spectra. We find that the last model in §3.3 above predicts quite well the amplitude (within 10%) of the OSSE spectrum. The model parameters are almost identical as for the model of the *ASCA* data alone (e.g., $W_b = 120$ eV) except that now the e-folding energy is fitted. The model P in Table 1 shows the parameters (here, the standard values of $\beta = 3$ and $r_{\text{in}} = 6$ have been assumed). For this model, we also study the

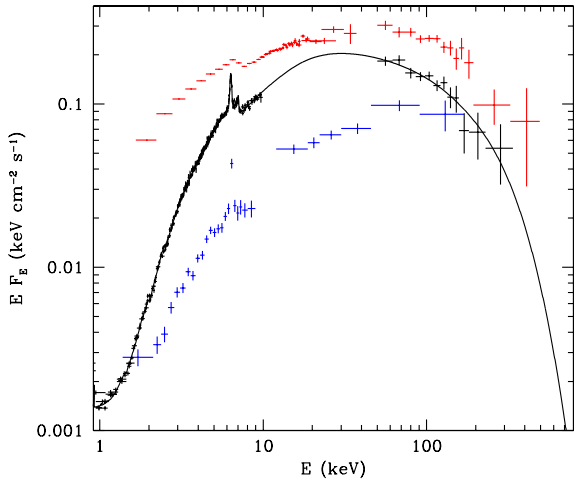


Fig. 4.— The *ASCA*-OSSE spectrum (black, middle), compared to the historical range (blue to red) of X-ray and soft γ -ray fluxes (highest and lowest X-rays from *Ginga* and *EXOSAT*, respectively, Z96; highest and lowest soft γ -rays from OSSE, J97, and *BeppoSAX*/PDS, P.-O. Petrucci, private communication, respectively). The solid curve gives the model with thermal Comptonization (§3.3).

allowed ranges of some parameters we otherwise keep fixed. We find the relative Fe abundance of $0.9_{-0.3}^{+0.2}$, and, importantly, the reflecting medium to be at most weakly ionized, with $\xi_{\text{refl}} = 1_{-1}^{+30}$ erg s $^{-1}$ cm, which range corresponds to the dominance of Fe I–XII, where effects of reflector’s ionization are negligible. In accordance with this result, increasing the disk line energy to 6.7 keV (Fe XXV–XXVI) leads to $\Delta\chi^2 = +18$, where we made conservative assumptions of a free i and Ω independent of W_b .

Next, we investigate a more physical model for the high energy spectrum. The high-energy cutoff of the OSSE data is strongly indicative of thermal Compton scattering, and the average OSSE spectrum of NGC 4151 can be well modelled by it (J97). An e-folded power law is only a rough approximation to spectra from that physical process. Thus, we now fit the spectrum with an isotropic Comptonization model (`compps` at <ftp://ftp.astro.su.se/pub/juri/XSPEC/COMPPS>) of Poutanen & Svensson (1996). The parameters of the thermal Compton continuum are the

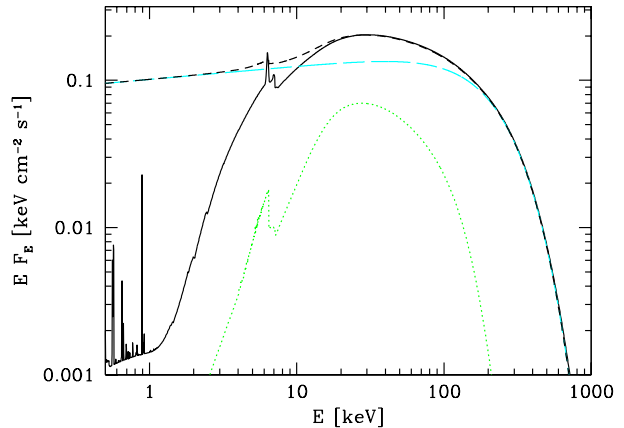


Fig. 5.— The components of the model with thermal Comptonization (solid curve). The short dashes show the intrinsic spectrum of the model with thermal Comptonization before absorption. The long dashes and dots give the Comptonization continuum and the reflection component together with the broad Fe K lines, respectively.

plasma temperature, kT , and the Compton parameter, $y \equiv 4\tau kT/m_e c^2$, where τ is the plasma Thomson optical depth. The assumption that the seed photons are blackbody at a temperature of 5 eV affects the resulting spectrum only very weakly. We find the absorber and the soft component parameters are virtually unchanged with respect to the previous model, but the reflection and disk line (with $W_b = 70$ eV) are somewhat weaker, see Table 1, model C. The normalization of the OSSE model with respect to that of SIS0 is close to unity (1.08), and the 2–10 keV index of the Comptonization component alone is $\Gamma = 1.89$. The spectrum is shown in Figure 4, together with the range of X-ray and soft γ -ray spectra historically observed from NGC 4151. Figure 5 shows the main components of the model.

For this model, we also consider the effect of allowing for variable β and r_{in} . We find that adding these two free parameters results only in a statistically insignificant reduction of χ^2 , by -3 . At this best fit, $\beta = 3.9$, $r_{\text{in}} = 6.3$, $W_b \simeq 60$ eV.

We also note that we find a bad fit of the thermal Compton model when we use the standard dual absorber model for the absorption ($\chi^2/\nu = 759/661$). Also, that model requires that the normalization of the OSSE spectrum is up by a fac-

tor of 2 with respect to that of the *ASCA* spectra. Thus, inclusion of the OSSE data provides further very strong support for the presence of complex absorption (with two partial-covering components). This result is in agreement with the OSSE spectra from NGC 4151 being consistent with thermal Comptonization with $\Gamma \simeq 1.9$ in X-rays (J97; Zdziarski et al. 2000).

The total intrinsic model luminosity is $L_{\text{bol}} = 3.9 \times 10^{43} \text{ erg s}^{-1}$, assuming isotropy and a distance of 13 Mpc. The emission measure of the optically-thin plasma is then $1.0 \times 10^{63} \text{ cm}^{-3}$, although we stress that we have approximated its emission as collisionally-ionized only (plus the 0.89-keV line) whereas Ogle et al. (2000) find evidence for both collisional ionization and photoionization. Our final models have the best-fit scattered fraction of $f_{\text{sc}} \simeq 1.5\%$ (see Table 1), which agrees with theoretical expectations of unified AGN models (Antonucci 1993). On the other hand, the corresponding model with the standard dual absorber has a higher value of $f_{\text{sc}} \simeq 3.5\%$.

3.5. Comparison with W99

W99 have studied a relatively small subset of the data considered here, namely the SIS data in the 1–10 keV range. Their model consists of the dual absorber, a power law component, Fe K disk and narrow lines from a neutral medium with both $K\alpha$ and $K\beta$ components, and an unabsorbed (scattered) power law. That last component is sufficient to model the soft excess in the considered energy range as most of its complexities appear below 1 keV (see §3.1), but we note it yields a rather high $f_{\text{sc}} \simeq 5\%$. W99 neglected reflection of the incident power law from the disk as they claimed there is no statistical evidence for its presence. We note, however, that this makes their model only a phenomenological description of the data, since their model assumes irradiation of a nearly-neutral, optically-thick, disk by the power-law source, and under these conditions a part of the irradiating photons *will* be Compton backscattered (see §3.2).

We have applied the same model to the SIS 1–10 keV data, and have closely reproduced their results of $\Gamma \simeq 1.30$ and $W_{\text{b}} \simeq 280 \text{ eV}$ at the best fit (with $\chi^2/\nu = 409/382$ with our binning and data reduction). At this χ^2 minimum, the width of the narrow line component is close to null. How-

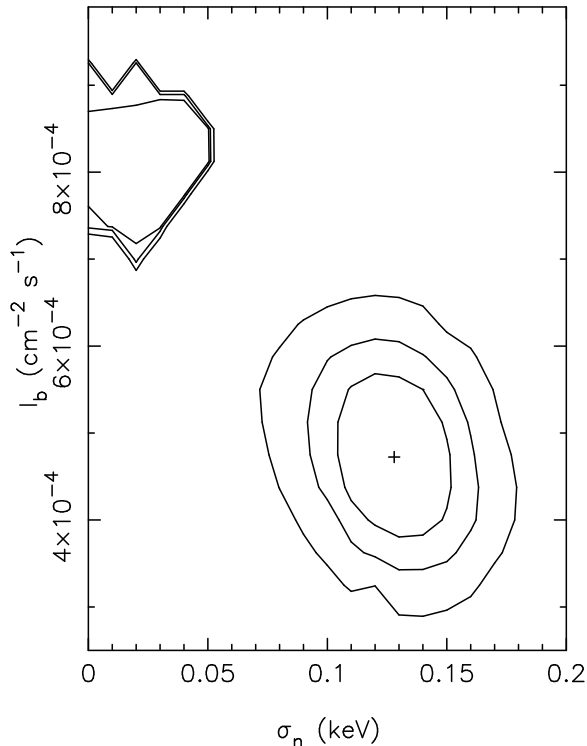


Fig. 6.— The contour plots (1, 2, and 3σ) of the photon flux in the disk line, I_{b} , vs. the width of the narrow line component, σ_{n} in the model with disk line only (W99), see §3.5. There exist two solutions with identical χ^2 , one with $\sigma_{\text{n}} \sim 0$ and a strong disk line, and one with $\sigma_{\text{n}} \sim 0.1 \text{ keV}$ and the disk line twice as weak. W99 have identified only the former.

ever, we find there exists another minimum with the same χ^2 , at which $W_{\text{b}} \simeq 150 \text{ eV}$ and the width of the narrow component is $\sigma_{\text{n}} \approx 0.1 \text{ keV}$, as illustrated in Figure 6. The uncertainties on W_{b} given by W99, $\pm 20 \text{ eV}$, appear to have been obtained under the assumption of $\sigma_{\text{n}} = 0$. However, as we discuss in §5 below, the presence of strong variable absorption in NGC 4151 implies the presence of Fe K emission of the absorbing clouds (Makishima 1986). If the clouds are at a plausible distance of $\sim 10^3 GM/c^2$ and cover $\gtrsim 10\%$ of the 4π solid angle (see §5), σ_{in} will be just $\sim 0.1 \text{ keV}$. Thus, the data used by W99 do allow the disk line to be substantially weaker than they claim.

On the other hand, the above ambiguity of spectral solutions disappears when the GIS 1–10

keV data are added. In that case, there is only *one* χ^2 minimum, which has $W_b \simeq 150$ eV and $\sigma_n \sim 0.1$ keV (similar to other models with disk line presented in this work), and setting $\sigma_n = 0.01$ keV results in $\Delta\chi^2 = +21$. Furthermore, when we add the data below 1 keV and model the soft excess in the same way as described in §3.1, we obtain $\chi^2/\nu = 720/636$ (at $\Gamma = 1.47^{+0.06}_{-0.04}$, $W_b = 110$ eV), which χ^2 is *higher* by 19 for the same number of degrees of freedom as in the corresponding model with reflection and dual absorber described in §3.2. Thus, the reprocessed/reflected component associated with the Fe K lines is not only needed physically but also *it is required statistically for our data*.

4. Variability

Overall, the total flux during the *ASCA* observation varied by $\sim 50\%$. The complexity of the spectrum indicated above was born out in the considerable spectral variability observed. The excess variance as a function of energy is shown in Figure 7. Below 1.5 keV the flux was constant, consistent with emission from an extended region. We note that, given the energy dependence of the variance shown in Figure 7, the average *ASCA* variance of the source is not a suitable quantity for comparison with other, much less absorbed Seyferts (Nandra et al. 1997). On the other hand, the excess variance in the 7–10 keV range, 7.5×10^{-3} , is most likely to represent the intrinsic source variability (although variability due to changes in the absorption cannot be ruled out completely). We have found this value to be fully consistent with variance of other broad-line Seyferts having intrinsic 2–10 keV luminosity of 1.4×10^{43} erg s $^{-1}$ (e.g. Leighly 1999), as illustrated in Figure 8. This tends to rule out the Compton mirror model proposed by Poutanen et al. (1996), which would predict a reduced amplitude of variability unless the mirror has the same size scale as the source.

Detailed analysis of the spectral variability is beyond the scope of this paper. However, we note that the highest amplitude of variability is in the 2.5–3.0 keV band. This increase with respect to the 7–10 keV one (likely to be mostly intrinsic) provides evidence for the importance of variability in the covering fraction/column density of the absorber in addition to the spectral in-

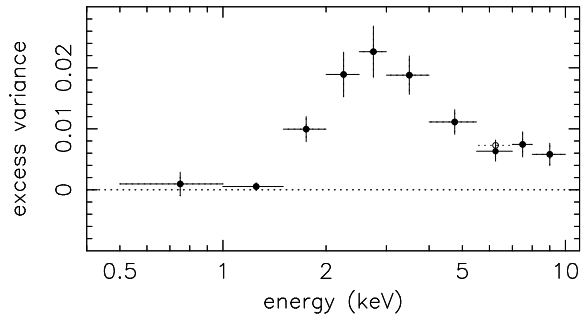


Fig. 7.— The fractional amplitude of intrinsic variability squared as a function of energy. The dotted symbol in the 5.5–7.0 keV band accounts for the constant narrow component of the emission line.

dex/intrinsic flux variability. We have confirmed that our physical model with complex absorption and disk line coupled to relativistically-broadened reflection also fits the time-resolved spectra. Thus, our fit results presented in §3 are not an artifact of time averaging.

The amplitude of variability is reduced in the 5.5–7.0 keV band compared with neighboring energies, as shown in Figure 7. This is most likely due to the contribution of the constant narrow component of the iron line, which contributes about 7% of the flux in that band, implying that the excess variance is a factor of 1.15 too low. Accounting for that makes excess variance in the 5.5–7.0 keV band comparable to that in the 7.0–8.0 keV band. The constant narrow component supports our two-component (narrow and disk) model of the iron line. The constancy of the narrow component of the line in this data set was first reported by Leighly et al. (1998).

5. The Narrow Line Component

The flux of the narrow $K\alpha$ component, $I_n \sim 2.5 \times 10^{-4}$ cm $^{-2}$ s $^{-1}$ in our best models (see Table 1; somewhat more in our other models), is higher than the flux of 1.8×10^{-4} cm $^{-2}$ s $^{-1}$ observed by *Chandra* in 2000 March (Ogle et al. 2000). Ogle et al. find that 65% of the line (i.e., $\sim 1.2 \times 10^{-4}$ cm $^{-2}$ s $^{-1}$) comes from kpc-scale gas. However, a part (dependent on the covering factor of the absorber) of the narrow line has to come from the absorbing medium (Makishima 1986),

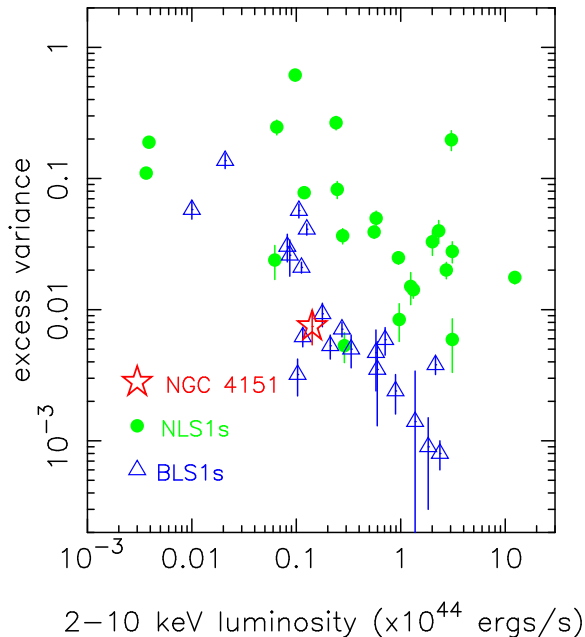


Fig. 8.— Comparison of the intrinsic X-ray variance of NGC 4151 with those of other broad and narrow-line Seyfert 1s (based on Leighly 1999). The intrinsic variance of NGC 4151 is rather typical for other broad-line Seyferts. Note that the decrease of the measured variance with increasing luminosity, L , appears to be an effect of the decreasing ratio of the typical length of an observation (limiting the range of timescales over which the variance is measured) to GM/c^3 at $M \propto L$. The data shown here are compatible with the *total* variance not showing any trend with L within each of the two types of Seyferts (e.g., Leighly 1999).

which medium is variable on long time scales (e.g., Yaqoob et al. 1993). We note that the optical flux peaked in 1995–1996, the U band magnitude had decreased by $\Delta M_U \approx 1.5$ by 2000 (Doroshenko et al. 2001), and the *Chandra* observation was made when NGC 4151 was in a low state. We suggest that the flux of the narrow component was higher during 1995 than it was in 2000 (consistent with a long-term variability of the soft excess, W94), and our results are consistent with those from *Chandra*. This is, in fact, confirmed by the findings of Weaver et al. (2001), who obtained $I_n \sim (3\text{--}4) \times 10^{-4} \text{ cm}^{-2} \text{ s}^{-1}$ in their fits to five *ASCA* observations of NGC 4151 (in X-ray high states). Also, the recent *XMM-Newton* result of Schurch

et al. (2002), who found $I_n \simeq 1.3 \times 10^{-4} \text{ cm}^{-2} \text{ s}^{-1}$ in a very low state of NGC 4151 (similar to the historically lowest state shown in Fig. 4) one year after the *Chandra* observation supports the picture of a part of the narrow line responding to changes of the intrinsic continuum.

The narrow component of the Fe K emission shows evidence of broadening, with $\sigma_n \simeq 0.05\text{--}0.1 \text{ keV}$ in our best models (see Table 1), and somewhat more in disk line models with the standard dual absorber in §3.2. This width is related to the velocity dispersion at the FWHM, $\Delta v = (8 \ln 2)^{1/2} (\sigma_n / E_{K\alpha}) c$ ($\lesssim 10^4 \text{ km s}^{-1}$ at the above σ_n). Roughly, Δv will be similar to the Keplerian velocity, which implies a characteristic radius where the emitting clouds are located of $R_c \sim 2 \times 10^3 GM/c^2$. These clouds are most likely the same clouds that absorb the intrinsic spectrum. As mentioned above, *Chandra* and *XMM-Newton* measured much narrower Fe K α lines at lower fluxes in later low states of NGC 4151 (Ogle et al. 2000). Thus, the “narrow” Fe K α line appears itself to consist of two components: one with $\sigma_n \ll 0.1 \text{ keV}$ originating in an extended region and constant on long time scales, and a component with $\sigma_n \sim 0.1 \text{ keV}$ emitted by the absorbing clouds and responding to variability of the nuclear source. However, given the *ASCA* resolution, using one Gaussian to represent both components of the narrow line is sufficient.

The characteristic line response time to changes in the nuclear continuum will be $\sim 2R_c/c$. For a fiducial $M = 10^7 M_\odot$, this gives $\sim 2 \times 10^5 \text{ s}$, consistent with the constancy (within the measurement errors) of the narrow line component during our observation (Leighly et al. 1998; see §4 above). On the other hand, variability of the absorber during the observation ($\sim 10^5 \text{ s}$) implies, assuming a cloud moving in the line of sight with the Keplerian velocity, the characteristic cloud size of a few times 10^{13} cm . This size should be similar to the size of the intrinsic X-ray source in order to allow it to partially cover our line of sight. This, in turn, is consistent with the size of the region where most of the gravitational energy is dissipated, $\sim 20GM/c^2$ or so.

The equivalent width of the narrow component with the parameters of Table 1 is $\sim 60 \text{ eV}$ with respect to other components of the observed absorbed spectrum. As calculated by Makishima

(1986), the equivalent width from an absorber completely surrounding a nuclear source would be ~ 300 eV at $N_{\text{H}} \sim 3 \times 10^{23} \text{ cm}^{-2}$ (as in Table 1). If a half of the observed I_{n} comes from the absorber (and the rest from the extended gas), $\sim 10\%$ or so of the lines of sight as seen from the nucleus should be covered by the clouds.

6. Discussion and Conclusions

We have performed a detailed and careful analysis of contemporaneous long observations of NGC 4151 by the *ASCA* and *CGRO* satellites in 1995. We find that proper inclusion of the Compton reflection component (taking into account its own relativistic smearing) associated with the broad Fe K line in the source is important for determination of the spectral index, Γ , of the power law component in this source. This component is required physically as well it is required statistically for our data (its inclusion results in a reduction of χ^2 by -20 without changing the number of free parameters). With it, $\Gamma \gtrsim 1.6$, which is within the 2σ range measured for Seyferts (Nandra & Pounds 1994). On the other hand, including Compton reflection has a little effect on the fitted parameters of the broad line.

Furthermore, we have studied the complexity of the absorber in this source. As previously noted by W94, the measured value of Γ depends crucially on the structure of the absorber. So far, the preferred model of the absorber has consisted of a uniform neutral screen and a partially-covering cloud (the dual absorber, e.g., W94). We have considered some simple and plausible modifications to this model. First, we confirm a finding by Piro et al. (2002) that the uniform screen is weakly ionized. Furthermore, we find very strong statistical evidence ($\sim 1 - 4 \times 10^{-6}$) for the presence of more than one partial-covering cloud in the line of sight. We find that the presence of the second absorbing cloud is not only strongly preferred statistically, but it also changes the fitted value of Γ to ~ 1.9 , close to the average index of Seyferts. In this model, the broad line component becomes relatively weak, with $W_{\text{b}} \sim 10^2$ eV (60–70 eV in our preferred physical model with thermal Comptonization). The corresponding reflection strength is $\Omega/2\pi \sim 1$, also average for Seyferts (Zdziarski et al. 1999). Our data also indicate that the broad

line component is dominated by the Fe K emission very close to the central black hole, similarly to the case of MCG -6-30-15 (Wilms et al. 2001).

Obviously, our model is not unique and, e.g., further complexity of the absorber is possible. One theoretical uncertainty involved regards the equivalent width of the Fe $K\alpha$ line with respect to the reflection continuum. Our choice of that quantity (1.3 keV) is based on George & Fabian (1991), whereas Życki & Czerny (1994) obtain values generally lower than 1 keV. Since our fits are driven by the line strength, the above choice is conservative in the sense that it gives the lowest theoretically predicted reflection strength. Adopting results of Życki & Czerny (1994) would yield values of Ω and Γ somewhat larger than those in Table 1.

Our model is consistent with a contemporaneous observation by the *CGRO/OSSE*. When the joint data are fitted by thermal Comptonization, the plasma temperature is ~ 70 keV, in the range of typical values for Seyferts (Zdziarski et al. 2000). We have also fitted data from *BeppoSAX* observations of NGC 4151 and have found excellent fits with the thermal-Compton model with two absorbing clouds and Compton reflection (work in preparation).

The finding that NGC 4151 appears to be an intrinsically average Seyfert 1 is also confirmed by comparison of its X-ray variance with that of other (optically) broad-line Seyferts. The crucial importance of complex absorption for the appearance of the X-ray spectra is further supported by the energy dependence of the variance, which peaks in the range where absorption of the intrinsic power law is the dominant effect.

We also have studied the narrow component of the Fe K emission. We find the presence of a broadened Gaussian component with $\sigma_{\text{n}} \sim 0.1$ keV or so in addition to the broad disk line. This allows us to construct a self-consistent scenario (§5) with Fe K emission of the absorbing clouds at a characteristic radius of a few thousands GM/c^2 . This moderately-broad component responds to changes of the nuclear continuum and thus was nearly absent during *Chandra* observation of NGC 4151 in a low state (Ogle et al. 2000).

This research has been supported by grants from KBN (5P03D00821, 2P03C00619p1,2), the

Foundation for Polish Science (AAZ) and NASA grant NAG5-9745 (KML, AAZ). Part of this work was done while KML was a STA fellow at RIKEN. We thank C. Done, T. Yaqoob, and the referee for valuable suggestions, and W. N. Johnson and P.-O. Petrucci for the OSSE and *BeppoSAX* data, respectively.

REFERENCES

- Abramowicz, M. A., Chen, X., Kato, S., Lasota, J.-P., & Regev, O. 1995, *ApJ*, 438, L37
- Anders, E., & Ebihara, M. 1982, *Geochim. Cosmochim. Acta*, 46, 2363
- Antonucci, R. R. J. 1993, *AAR&A*, 31, 473
- Arnaud, K. A. 1996, in *ASP Conf. Series 101, Astronomical Data Analysis Software and Systems V*, ed. G. H. Jacoby & J. Barnes (San Francisco: ASP), 17
- Chiang, J., Reynolds, C. S., Blaes, O. M., Nowak, M. A., Murray, N., Madejski, G. M., Marshall, H. L., & Magdziarz, P. 2000, *ApJ*, 528, 292
- Done, C., Mulchaey, J. S., Mushotzky, R. F., & Arnaud, K. A. 1992, *ApJ*, 395, 275
- Done, C., Madejski, G. M., & Życki, P. T. 2000, *ApJ*, 536, 213
- Doroshenko, V. T., et al. 2001, *Ast. L.*, 27, 65
- Fabian, A. C., Rees, M. J., Stella, L., & White, N. E. 1989, *MNRAS*, 238, 729
- George, I. M., & Fabian, A. C. 1991, *MNRAS*, 249, 352
- George, I. M., Turner, T. J., Netzer, H., Nandra, K., Mushotzky, R. F., & Yaqoob, T. 1998, *ApJS*, 114, 73
- Gilfanov, M., Churazov, E., & Revnivtsev, M. 2000, in *Proc. 5th CAS/MPG Workshop on High Energy Astrophysics*, ed. G. Zhao et al. (Beijing: China Sci. Techn. Press), 114 (astro-ph/0002415)
- Haardt, F. 1993, *ApJ*, 413, 68
- Johnson W. N., McNaron-Brown, K., Kurfess, J. D., Zdziarski, A. A., Magdziarz, P., & Gehrels, N. 1997, *ApJ*, 482, 173 (J97)
- Leighly, K. M., 1999, *ApJS*, 125, 297
- Leighly, K. M., Cappi, M., Matsuoka, M., & Mihara, T., 1997, in *X-ray Imaging and Spectroscopy of Cosmic Hot Plasmas*, ed. F. Makino & K. Mitsuda (Tokyo: Universal Academy Press), 291
- Leighly, K. M., Matsuoka, M., Cappi, M., & Mihara, T., 1998, in *The Hot Universe*, ed. K. Koyama, S. Kitamoto, M. Itoh (Dordrecht: Kluwer Academic), 422
- Lightman, A. P., & Zdziarski A. A. 1987, *ApJ*, 319, 643
- Lubiński, P., & Zdziarski, A. A. 2001, *MNRAS*, 323, L37
- Magdziarz, P., & Zdziarski, A. A. 1995, *MNRAS*, 273, 837
- Makishima, K., 1986, in *The Physics of Accretion onto Compact Objects*, ed. K. O. Mason, M. G. Watson, & N. E. White (Berlin: Springer), 249
- Mewe, R., Gronenschild, E. H. B. M., & van den Oord, G. H. J., 1985, *A&AS*, 62, 197
- Murphy, E. M., Lockman, F. J., Laor, A., & Elvis, M. 1996, *ApJS*, 105, 369
- Nandra, K., & Pounds, K. 1994, *MNRAS*, 268, 405
- Nandra, K., George, I. M., Mushotzky, R. F., Turner, T. J., & Yaqoob, T. 1997, *ApJ*, 476, 70
- Narayan, R., & Yi, I. 1995, *ApJ*, 452, 710
- Ogle, P. M., Marshall, H. L., Lee, J. C., & Canizares, C. R. 2000, *ApJ*, 545, L81
- Piro, L., Nicastro, F., Perola, G. C., Capalbi, M., Cappi, M., Grandi, P., Maraschi, L., & Petrucci, P. O. 2002, *A&A*, submitted
- Poutanen, J. 1998, in *Theory of Black Hole Accretion Discs*, ed. M. A. Abramowicz, G. Björnsson, & J. Pringle, (Cambridge: Cambridge Univ. Press), 100 (astro-ph/9805025)
- Poutanen, J., Sikora, M., Begelman, M. C., Magdziarz, P., 1996, *ApJ*, 465, 107
- Poutanen, J., & Svensson, R. 1996, *ApJ*, 470, 249
- Schurch, N. J., Warwick, R. S., Griffiths, R. E., & Ptak, A. F. 2002, in *New Visions of the X-ray Universe in the XMM-Newton and Chandra Era*, ed. F. Jansen et al., ESA SP-488, in press
- Sunyaev, R. A., & Titarchuk, L. G. 1980, *A&A*, 86, 121
- Wang, J.-X., Zhou, Y.-Y., & Wang T.-G. 1999, *ApJ*, 523, L129 (W99)
- Warwick, R. S., Done, C., & Smith, D. A. 1995, *MNRAS*, 275, 1003
- Weaver, K. A., Yaqoob, T., Holt, S. S., Mushotzky, R. F., Matsuoka, M., & Yamauchi, M. 1994, *ApJ*, 436, L27 (W94)
- Weaver, K. A., Gelbord, J., & Yaqoob, T. 2001, *ApJ*, 550, 261
- Wilms, J., Reynolds, C. S., Begelman, M. C., Reeves, J., Molendi, S., Staubert, R., & Kendziorra, E. 2001, *MNRAS*, 328, L27
- Yang, Y., Wilson, A. S., & Ferruit, P. 2001, *ApJ*, 563, 124
- Yaqoob, T., & Warwick, R. S. 1991, *MNRAS*, 248, 773
- Yaqoob, T., Warwick, R. S., Makino, F., Otani, C., Sokoloski, J. L., Bond, I. A., & Yamauchi, M. 1993, *MNRAS*, 262, 435
- Yaqoob, T., Edelson, R., Weaver, K. A., Warwick, R. S., Mushotzky, R. F., Serlemitsos, P. J., & Holt, S. S. 1995, *ApJ*, 453, L81
- Zdziarski, A. A. 2000, in *IAU Symp. 195, Highly Energetic Physical Processes and Mechanisms for Emission from Astrophysical Plasmas*, ed. P. C. H. Martens, S. Tsuruta & M. A. Weber (San Francisco:

ASP), 153 (astro-ph/0001078)
Zdziarski, A. A., Johnson, W. N., & Magdziarz, P.
1996, MNRAS, 283, 193 (Z96)
Zdziarski, A. A., Lubiński, P., & Smith, D. A. 1999,
MNRAS, 303, L11
Zdziarski, A. A., Poutanen, J., & Johnson, W. N.
2000, ApJ, 542, 703
Życki, P. T., & Czerny, B. 1994, MNRAS, 266, 653
Życki, P.T., Done, C., Smith, D.A. 1998, ApJ, 496,
L25

TABLE 1
REST-FRAME MODEL PARAMETERS OF THE BROAD-BAND SPECTRUM

	N_0	ξ	N_1	f_1	N_2	f_2	E_c, kT	Γ, y	$\Omega/2\pi$	f_{sc}	kT_s	E_n	σ_n	I_n	χ^2/ν
P	$3.7^{+0.4}_{-0.5}$	$0.37^{+0.27}_{-0.29}$	28^{+6}_{-6}	$0.40^{+0.06}_{-0.08}$	$6.0^{+0.7}_{-0.7}$	$0.77^{+0.05}_{-0.04}$	210^{+100}_{-60}	$1.87^{+0.07}_{-0.08}$	$0.95^{+0.29}_{-0.30}$	0.016	$0.16^{+0.02}_{-0.02}$	$6.36^{+0.02}_{-0.02}$	$0.07^{+0.02}_{-0.04}$	$2.4^{+0.3}_{-0.3}$	682/658
C	$3.8^{+0.3}_{-0.5}$	$0.41^{+0.34}_{-0.28}$	32^{+5}_{-6}	$0.44^{+0.05}_{-0.07}$	$6.1^{+0.6}_{-0.6}$	$0.78^{+0.04}_{-0.05}$	73^{+34}_{-29}	$0.88^{+0.12}_{-0.11}$	$0.60^{+0.24}_{-0.21}$	0.014	$0.16^{+0.02}_{-0.02}$	$6.35^{+0.02}_{-0.02}$	$0.08^{+0.02}_{-0.03}$	$2.6^{+0.4}_{-0.2}$	682/658

NOTE.—Model P is a phenomenological model with an e-folded power law while model C is a physical Comptonization model. N , the ionization parameter ξ , I_n , and (kT , E_c , E_n , σ_n) are in units of 10^{22} cm $^{-2}$, erg s $^{-1}$ cm, 10^{-4} cm $^{-2}$ s $^{-1}$, and keV, respectively.